ELSEVIER

Surface Science 432 (1999) 245–256

surface science

www.elsevier.nl/locate/susc

Electronic and vibrational electron energy loss studies of the formation of SiO_2 and carbonaceous layers on Si(111)7 × 7 by thermal and ion-assisted deposition techniques

H. Yu, K.T. Leung *

Department of Chemistry, University of Waterloo, Waterloo, Ontario N2L 3G1, Canada

Received 25 January 1999; accepted for publication 30 March 1999

Abstract

Electronic and vibrational electron energy loss spectroscopy (EELS) and Auger electron spectroscopy (AES) were used to characterize the formation of SiO_2 and SiC on Si(111)7 × 7. The differences between thermal deposition and ion-assisted deposition of these films were investigated. Thermally formed SiO_2 layers obtained by annealing the silicon sample in O_2 at 700 K can be characterized by the electronic transitions near 5 and 7 eV and by the blue shifts in its vibrational features from that of atomic oxygen adsorption. The formation of SiO_2 could also be achieved by ion irradiation at room temperature (RT). Carbonaceous layers formed at different ethylene dosages and sample temperatures were characterized by EELS and AES. Like the oxide formation, a higher efficiency in producing the carbonaceous layer was obtained by using ion-assisted deposition than thermal deposition. In particular, a SiC layer could be obtained by cycles of ethylene ion irradiation at RT and annealing to 800 K, whereas a very large dosage of ethylene ions at RT was found to produce a graphite layer.

Keywords: AES; Carbonaceous layers; EELS; Si(111)7 × 7; Ion irradiation; SiO_2; SiC

1. Introduction

Both oxide and carbide layers are among the most common types of thin films found on silicon surfaces. The natures of the oxidation layer and its formation mechanisms on different low Miller index planes of Si have been studied extensively over the past three decades. Although the details of the initial molecular adsorption are under intense debates [1–3], it has generally been accepted that oxygen exposure to a Si surface at room temperature (RT) would lead to the breakage of a Si—Si bond via the insertion of an atomic oxygen between two Si atoms [4,5]. Unlike the vitreous SiO_2 structure in silica with a Si—Si separation of 3.05 Å, the Si—Si separation in the oxide layer formed on a silicon surface at RT is essentially the same as that in crystalline silicon (2.35 Å) [4]. This oxide layer therefore has a smaller bond angle (the angle between two S—O bonds) than that in the vitreous SiO_2 structure and has been described as a 'compressed' SiO_2 structure by Ibach et al. [4]. The vitreous SiO_2 layer was not found on Si(111)7 × 7 for oxygen exposure even as high as 10^{11} L at RT, but it could be formed if the Si sample was held at 700 K during the O_2 exposure [4]. Hollinger et al. [6] showed that the formation of SiO_2 films involves an evolution of chemical structure from a metasta-

* Corresponding author. Fax: +1-519-746-0435.
E-mail address: tong@uwaterloo.ca (K.T. Leung)

0039-6028/99/$ – see front matter
PII: S0039-6028(99)00545-2

ble random bonding phase to a microscopic mixture of Si and SiO_2 when the sample temperature is increased. Furthermore, the uptake rate at a higher temperature ($\sim$970 K) was found to be enhanced in the high-exposure region but was significantly reduced in the low-exposure region, which could be due to oxygen desorption as volatile SiO [6]. Whereas Ibach and coworkers have examined the SiO_2 layer by using electron energy loss spectroscopy (EELS) in a second derivative mode [7], the characterization of SiO_2 films by EELS in the normal (i.e. non-derivative) mode, which generally provides a more straightforward elucidation into the nature of this material, has not been reported. Furthermore, although thermally formed SiO_2 layers have been investigated extensively, no study on the ion-assisted formation of SiO_2 has been carried out.

Another widely investigated film on silicon surfaces is the carbonaceous film. Depending on the deposition procedures used, there are different kinds of carbonaceous films that can be formed on a silicon surface, including SiC, graphite, amorphous C, amorphous C:H, diamond-like carbon, and diamond films [8,9]. These films are usually grown by chemical vapor deposition, together with various kinds of reaction enhancement techniques involving ion-sputtering and other plasma-assisted methods. The nature of these films is usually defined by the relative content of sp^3 tetrahedrally coordinated carbon and the concentration of atomic hydrogen in the films. Although a large amount of work has been devoted to the preparation of these films involving different methods and recipes [10], detailed understanding of the growth mechanisms and the initial reaction process is far from complete, especially for the complicated ion or plasma assisted processes [11,12]. In-situ studies on the early stages in the formation of these films will therefore be of great interest.

Because of its capability in providing distinct information about electronic transitions and plasmon excitations, EELS has evolved as a powerful tool for the characterization of thin films [8,13]. Depending on the impact energy and the scattering geometry employed in the inelastic electron surface scattering process, the incident electron can be manipulated to penetrate the film to different depths into the surface region. It is therefore possible to obtain information about the electronic structures of both the surface and the sub-surface region (approximately 2–6 monolayers below the topmost layer for an impact energy of 20–1000 eV) [14,15]. Although EELS spectra collected in the second derivative mode can be used to reveal the more prominent changes in the peak shapes of the observed EELS features [7], EELS spectra recorded in the normal (non-derivative) mode offer more direct and meaningful measurements of the energy positions of the peak maxima and the relative intensities of individual peaks. In the present work, we apply EELS measurements in the non-derivative mode both over an extended range and at high resolution, along with Auger electron spectroscopy (AES), to investigate the initial formation of SiO_2 and SiC layers on a $Si(111)7\times7$ surface by thermal and ion irradiation methods.

2. Experimental

Details of the experimental apparatus used in the present work have been described previously [16]. Briefly, all the experiments were performed in a home-built ultra-high-vacuum chamber with a base pressure of better than 1×10^{-10} Torr, achieved by a 170 $\ell\,s^{-1}$ turbomolecular pump, a 230 $\ell\,s^{-1}$ ion pump and a 2000 $\ell\,s^{-1}$ titanium sublimation pump. The chamber was equipped with an ion(-sputtering) gun, a four-grid retarding-field optics for both reverse-view low-energy electron diffraction (LEED) and AES analyses, a 1–300-amu quadrupole mass spectrometer (QMS) for temperature-programmed desorption studies, and a home-built multi-technique electron spectrometer for both electronic and vibrational EELS measurements. The QMS was housed in a separate chamber that was differentially pumped by a 60 $\ell\,s^{-1}$ ion pump. Details of our EELS spectrometer have also been described in Ref. [17]. In the high-resolution mode, our EELS spectrometer is capable of an optimal energy resolution of 6.5 meV (45 cm^{-1}) full-width at half-maximum (FWHM), with a count-rate over 100 000 counts per second for the elastic peak, at a typical (low) impact energy of 4 eV. In the high impact energy

mode used for electronic EELS measurements, the energy resolution becomes 30 meV FWHM, which is considerably better than the performance of most commercially available spectrometers. Our spectrometer therefore offers adequate performance for most of our applications, covering both the vibrational studies at high resolution and the electronic structural investigations over an extended energy loss range.

The Si(111) sample (p-type boron doped, $50\ \Omega\cdot$cm, $8\times6\ \text{mm}^2\times0.5$ mm thick) with a stated purity of 99.999% was obtained commercially. The sample was mechanically fastened to a grounded Ta sample plate with 0.25-mm-diameter Ta wires. Heating of the Si sample was achieved by electron bombardment from a heated tungsten filament at the backside of the sample. The Si(111) sample was cleaned by using a standard procedure involving repeated cycles of Ar^+ sputtering and annealing to 1200 K, until a sharp 7×7 LEED pattern and no detectable Auger peaks attributable to C, O and S were obtained. The cleanliness of the sample was further confirmed by the lack of detectable vibrational EELS features attributable to unwanted contaminants. The commercial gaseous samples, ethylene and oxygen (all at 99.99% purity), were used without further purification.

Ion irradiation (without mass selection) was performed by operating the ion gun with the chamber back-filled with the gas of interest at a typical ambient pressure of 1×10^{-6} Torr. The sample was positioned 5 cm from the front face of the ion gun during the ion irradiation experiments. The impact energy of the ion beam could be controlled by adjusting a floating voltage applied on the sample with respect to a pre-selected beam energy of the ion gun. The ion dose can be estimated by the product of the ion flux (~10 nA mm^{-2}) and the exposure time [obtained from the exposure in units of Langmuir ($1\ \text{L}=1\times10^{-6}$ Torr$\cdot$s) and the pressure employed (1×10^{-6} Torr)]. In the present experimental set-up, the reactant gases were ionized by electrons with 200 eV kinetic energy inside the ion gun, and only positive ions from the ion gun could reach the sample without mass selection. The concentration of each ion can be estimated from its cracking pattern [18]. For example, in the case of ethylene, the parent ion $C_2H_4^+$ is also the majority base ion, with other smaller ions such as $C_2H_3^+$, $C_2H_2^+$, C_2H^+, CH_2^+, and CH^+ present with decreasing concentrations. When the ions collide with the surface, they may become neutralized and/or undergo further dissociation into other smaller ionic or neutral fragments including atomic carbon and hydrogen. The resulting species may also subsequently react with the substrate atoms and/or other pre-deposited adsorbates.

3. Results and discussion

3.1. Formation of SiO_2 on Si(111) 7×7

Previous studies by Ibach and Rowe on clean Si(111)7×7 by using EELS in a second derivative mode [7] revealed several interesting spectroscopic features, including a bulk plasmon at ~17 eV, a surface plasmon at 10 eV, three surface-related transitions at 1.8, 8, and 15 eV, and two bulk band transitions at 3 and 4.5 eV. A later study involving normal-mode EELS by Froitzheim et al. [19] also reported the surface and bulk transitions below 6 eV, which were found to be less evident than the corresponding features found in the second-derivative-mode EELS study [7]. Fig. 1 shows our normal-mode EELS spectra for clean Si(111)7×7 before and after 1 kL (1 kL = 1000 L) of oxygen exposure held at RT, 550 and 700 K. The previously reported features for the bulk plasmon at 17.5 eV, surface plasmon at 10 eV (appeared as a shoulder), and surface-related transition at 1.8 eV on clean Si(111)7×7 are clearly evident in Fig. 1a. Other features found by the second-derivative-mode EELS [7] are not observed in our normal-mode EELS spectra. Our results are, however, consistent with the results obtained by using normal-mode EELS reported by other groups [8,15,20]. After a 1 kL of oxygen exposure at RT, the surface-related transition at 1.8 eV disappeared, and no additional EELS feature was found (Fig. 1b). The plasmon features (at 10 and ~17 eV) became broadened due to dissociative adsorption of atomic oxygen. Although the previous EELS study using the second derivative mode [7] also indicated an increase in the intensities of

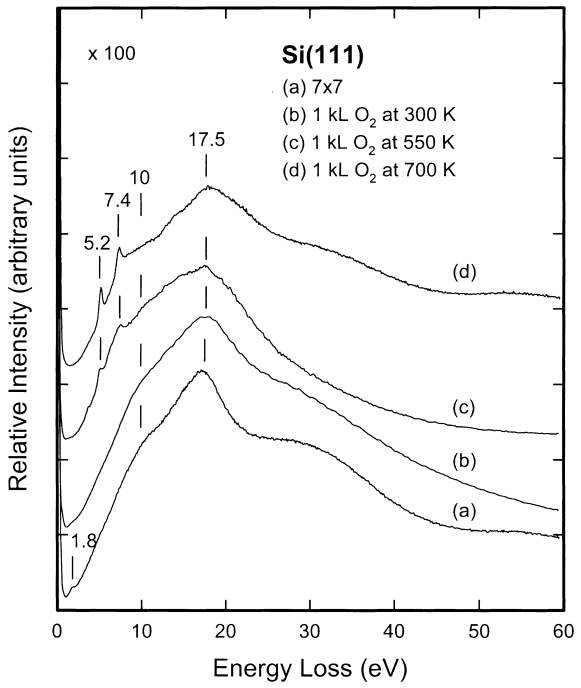

Fig. 1. Electronic electron energy loss spectra for (a) clean Si(111)7×7, and after exposure of 1 kL of oxygen with sample (a) held at (b) 300 K, (c) 550 K, and (d) 700 K.

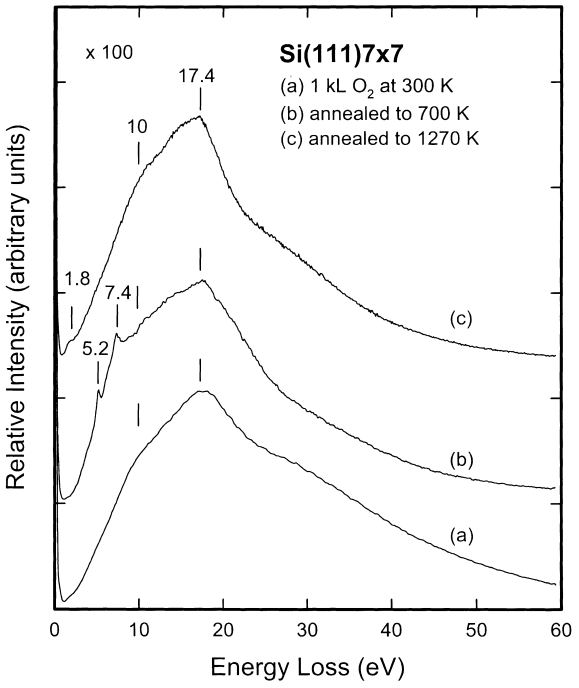

Fig. 2. Electronic electron energy loss spectra for Si(111)7×7 with (a) 1 kL oxygen exposure at 300 K, and followed by annealing to (b) 700 K, and (c) 1270 K.

the features at 5.2 and 7.4 eV after the dosing of oxygen, these changes are less apparent in our normal-mode spectra. When the oxygen exposure was performed with the sample held above 550 K (Fig. 1c and d), two sharp peaks appeared at 5.2 and 7.4 eV. Previous studies showed that at an elevated temperature, the chemical composition of the oxidation products changes from a metastable random bonding phase to a mixture of Si and SiO_2 accompanied by the enhancement of oxidation [1,6,21]. Clearly, the two peaks observed at 5.2 and 7.4 eV can be assigned to transitions related to SiO_2. It is also unlikely that these two peaks were simply caused by an increase in the surface oxygen concentration because a separate experiment involving a significantly higher exposure of 10 kL oxygen to Si(111)7×7 at RT did not produce these peaks. Furthermore, if the sample in Fig. 1b (also shown in Fig. 2a) was annealed from RT to a higher temperature (700 K), the resulting sample also exhibited the two peaks at 5.2 and 7.4 eV (Fig. 2b), which suggests that these two peaks are related to the bonding structure of SiO_2. The formation of SiO_2 at 700 K is also consistent with the corresponding vibrational EELS spectrum shown in Fig. 3b for a sample prepared with a similar O_2 exposure. In particular, blue shifts as a result of increased lateral interactions and surface structural rearrangement [22] were found in the characteristic frequencies at 378, 716, and 1030 cm^{-1} (Fig. 3a) for the rocking, symmetric and asymmetric stretching modes of the Si—O—Si radical, respectively [4]. No LEED pattern was observed for both samples shown in Fig. 3, which indicates that oxygen atoms are randomly adsorbed on the surface (i.e. without any long range order). When the sample after the 700 K anneal (Fig. 2b) was further annealed to 1270 K (Fig. 2c), oxygen or oxygen-containing species were found to desorb from the surface. The EELS spectrum of the resulting sample (Fig. 2c) essentially reverted back to that of a clean surface (Fig. 1a), and the 7×7 LEED pattern was restored.

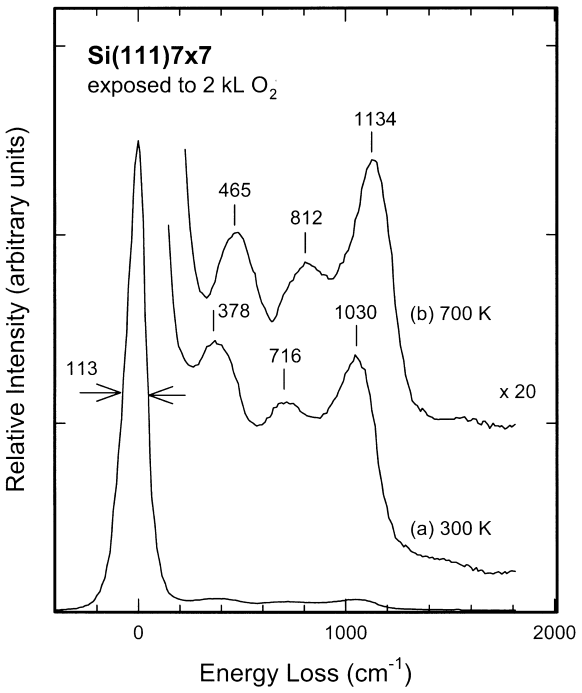

Fig. 3. Vibrational electron energy loss spectra for 2 kL of oxygen exposed to Si(111)7×7 at (a) 300 K, and (b) 700 K.

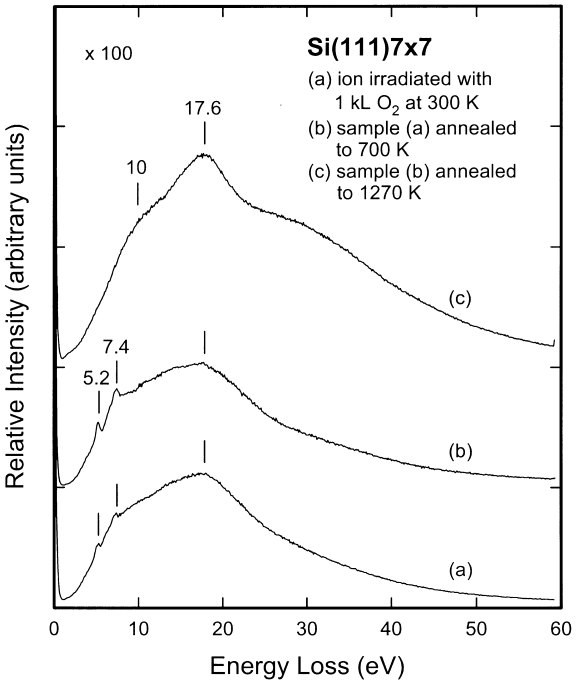

Fig. 4. Electronic electron energy loss spectra for Si(111)7×7 (a) ion-irradiated with 1 kL of oxygen at 200 eV impact energy at 300 K, and followed by annealing to (b) 700 K, and (c) 1270 K.

Although a large dose of oxygen at RT does not generate SiO_2 on the silicon surface [4], SiO_2 can be produced non-thermally by ion-assisted deposition at RT. Fig. 4 shows the electronic EELS spectra for Si(111)7×7 ion-irradiated in O_2 at 200 eV impact energy and 10 nA mm^{-2} at RT, following the procedure described above. In particular, Fig. 4a clearly depicts the presence of SiO_2 on the surface, although the features at 5.2 and 7.4 eV are not as intense as those found for the sample prepared at the same oxygen exposure without ion irradiation at 700 K (Fig. 1d). Annealing the sample in Fig. 4a to a higher temperature (700 K) increased the intensities of the peaks at 5.2 and 7.4 eV (Fig. 4b), which indicates that the initial products after ion irradiation contained both adsorbed atomic oxygen and SiO_2. As the temperature was increased to 700 K, the adsorbed atomic oxygen apparently underwent transformation to SiO_2, hence increasing its concentration. Finally, when the sample was further annealed to 1270 K (Fig. 4c), all the surface oxygen desorbed, and the sharp 7×7 LEED pattern was again restored. Because the formation of SiO_2 requires the breakage of the Si–Si bonds and the dislocation of the Si atoms in the sub-surface region, this experiment therefore provides evidence for ion-induced rearrangement of surface atoms to form SiO_2 at RT.

3.2. Formation of a carbonaceous layer on Si(111)7×7

Electronic EELS has proven to be a useful tool for probing plasmon excitations of C-containing thin films [8,15]. In particular, films with a sp^3 bonding structure such as diamond and SiC can be identified by the characteristic energy positions of their surface and bulk plasmon peaks. For films involving a sp^2 bonding structure (such as graphite, *a*-C, and *a*-C:H), their corresponding plasmon features include a π plasmon due to the π electrons and a π+σ plasmon due to the valence electrons

Table 1
Energy positions and the relative sp^2 and sp^3 C-bond contents for the plasmon features commonly found in carbon-containing films (from Refs. [8,15,24])

	Energy position (eV)				Percentage of sp^2 or sp^3 C-bonds to the total C-bonds
	Surface plasmon	Bulk plasmon	π plasmon	$\pi+\sigma$ plasmon	
Graphite	–	–	7	25	100 sp^2
a-C	–	–	6	23	80 ± 10 sp^2
a-C:H	–	–	6	25	40 ± 5 sp^2
β-SiC	18	23	–	–	100 sp^3
Diamond	24	33	–	–	100 sp^3

[8,23]. Table 1 summarizes the typical energy positions of these plasmon features for different carbonaceous films reported in the literature [8,15,24]. The films are identified by the percentage content of the sp^2 or sp^3 bond with respect to the total carbon bonds in the corresponding films.

Carbon can be deposited on Si(111)7×7 simply by annealing the sample in ethylene at 800 K. Although a small amount of surface carbon ($<5\%$) is difficult to detect by our present AES setup involving a retarding field analyser, its presence can be easily verified by vibrational EELS by means of the characteristic Si—C stretching vibration at 800 cm^{-1} [4]. Previous studies by Yates and coworkers [15,25] indicated that only a limited amount of carbon could be deposited on a Si(100) surface below 940 K due to a diffusion-limited growth mechanism, which suggests that in this 'lower' temperature range, the limited lattice mobility prevents the formation of SiC. In order to determine the properties of the thermally deposited carbonaceous layer, we performed a series of vibrational EELS and AES experiments at different ethylene dosages (Figs. 5 and 6). Fig. 5 shows the vibrational EELS spectra for a sample annealed with two typical dosages (50 L and 2 kL) of ethylene at 800 K. The strengthening of the peak at 826 cm^{-1} in Fig. 5b and c clearly indicates the increase in the carbon concentration. The new peak at 1714 cm^{-1} (Fig. 5c) corresponds to an overtone of the Si—C stretch at 826 cm^{-1}. As the dosage was increased to 2 kL, the corresponding LEED pattern changed from a sharp 7×7 pattern to diffuse 7×7, 1×1, and finally to a very diffuse 1×1 pattern. The carbonaceous layer so produced

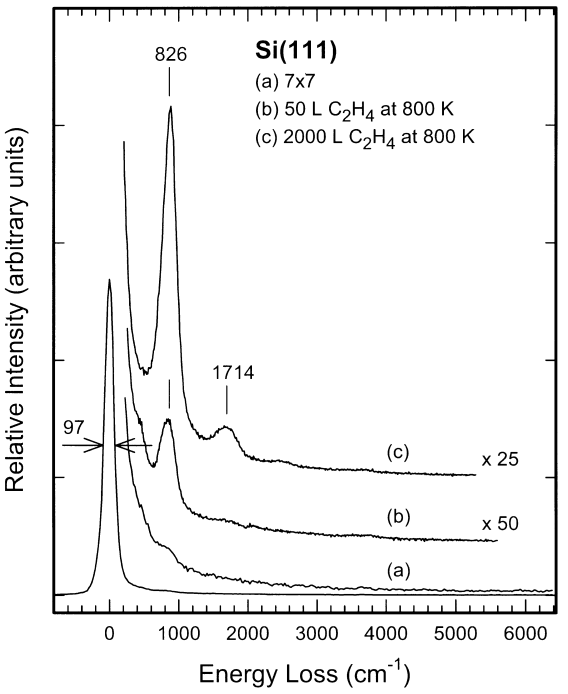

Fig. 5. Vibrational electron energy loss spectra for (a) clean Si(111)7×7 exposed with (b) 50 L, and (c) 2000 L of ethylene at 800 K.

was clearly disordered and may be described as a thin Si–C alloy layer containing a random mixture of C and Si atoms, as proposed in an earlier study on Si(100) by Bozso et al. [15]. Annealing this C-covered surface to a higher temperature (1200 K) could reduce the surface carbon feature (at 826 cm^{-1}) and partially restore the 7×7 LEED pattern, which indicates carbon diffusion into the

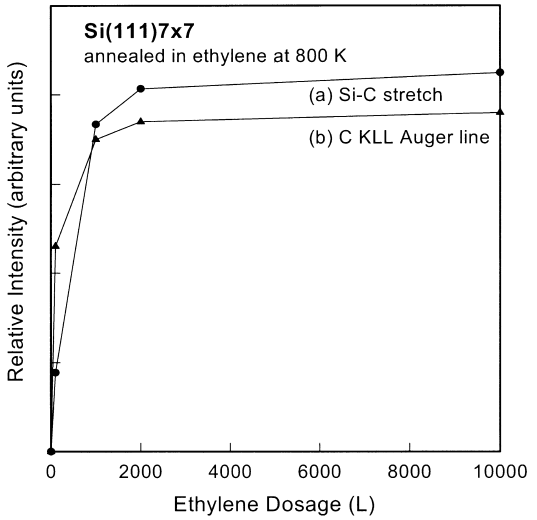

Fig. 6. Relative intensity of a carbon-related feature for Si(111)7×7 annealed at 800 K as a function of ethylene dose in (a) a vibrational EELS spectrum (the Si—C stretch at 826 cm^{-1} energy loss), and (b) an AES spectrum (the C KLL Auger transition at 274 eV electron energy).

bulk. The present result is also consistent with that observed on Si(100) [15].

In Fig. 6, we show the relative intensities of representative carbon-related features observed in the vibrational EELS and AES spectra as a function of ethylene exposure to Si(111)7×7 held at 800 K. In particular, the peak at 826 cm^{-1} corresponding to Si—C stretch (as shown in Fig. 5) was used for the vibrational EELS spectra (Fig. 6a), whereas the carbon KLL Auger transition at 274 eV was used for the AES spectra (Fig. 6b). Both curves show that the carbon concentration increases rapidly below 1 kL of ethylene exposure and becomes saturated above 2 kL. Because the vibrational EELS spectra contain information primarily about the surface region, and AES spectra contain contributions from both the surface and the sub-surface, the intensities of the EELS and AES features are expected to level off at different ethylene dosages if the surface carbon atoms were to keep diffusing into the bulk. The similarity in the intensity variations for both the EELS and AES features indicates that carbon diffusion into the bulk is not a dominant process at this temperature, which is consistent with the Si(100) result reported by Bozso et al. [15]. Moreover, further annealing the C-covered surface to a higher temperature (>1000 K) reduced the intensities of the corresponding carbon-related features in both the EELS and AES spectra (not shown), which suggests that significant diffusion of carbon atoms into the bulk occurs at a higher temperature.

To further characterize the thermally deposited carbonaceous layer by means of its characteristic plasmon and electronic excitations, electronic EELS experiments were conducted. Fig. 7 shows the electronic EELS spectra of Si(111)7×7 before and after annealing the sample in 1 and 10 kL of ethylene at 800 K. With increasing ethylene dosage, the surface plasmon at 10 eV became less evident and the bulk plasmon peak for the clean surface shifted from 17.4 eV (Fig. 7a) to 20 eV after the 10 kL ethylene dosage (Fig. 7c). The broad peak observed at 20 eV could be attributed to the existing Si bulk plasmon peak at ~17 eV (Fig. 7a) with an additional contribution from the $\pi+\sigma$ plasmon for *a*-C at 23 eV (Table 1). Because

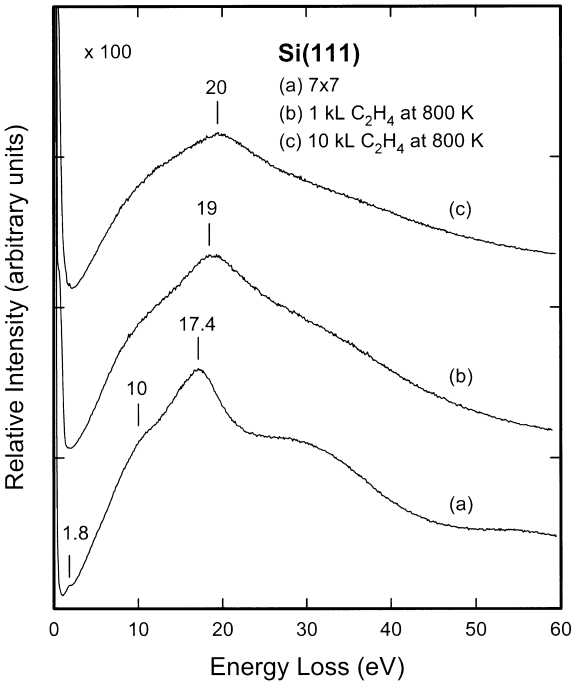

Fig. 7. Electronic electron energy loss spectra for (a) clean Si(111)7×7 exposed with (b) 1 kL, and (c) 10 kL of ethylene at 800 K.

the bulk plasmon peak of SiC was also found to be at 23 eV (Table 1), the presence of SiC cannot be ruled out. A similar feature has also been found on Si(100) obtained by using a molecular beam chemical vapour deposition technique, and the corresponding as-formed layer was assigned as a 'Si–C alloy' [15]. Bozso et al. [15] also suggested that the formation of SiC occurred below the top Si layer at a higher annealing temperature ($\sim$940 K). Because the impact energy used in our present electronic EELS setup was limited to 100 eV, we could not detect the formation of SiC in the silicon sub-surface region due to the limited electron penetration depth [15]. After annealing the sample in Fig. 7c to a higher temperature (>1200 K), we observed that the plasmon peak shifted back to 18 eV (not shown), consistent with carbon diffusion into the bulk and partial restoration of the 7×7 surface, as discussed earlier.

At RT, ethylene was reported to adsorb molecularly on the Si(111) surface with near sp^3 hybridization by Yoshinobu et al. [26]. However, with the irradiation of unmass-selected ethylene ions, adsorption of hydrocarbon species was found to occur considerably more efficiently. The vibrational EELS features of the corresponding adsorbed species were evidently different from that of the molecularly adsorbed ethylene. Fig. 8 compares the vibrational EELS spectra for the adsorption of ethylene with and without ion irradiation on Si(111)7×7 at RT. In particular, the C—H stretch observed at 2911 cm^{-1} for Si(111)7×7 exposed with 1 kL of ethylene at RT (Fig. 8a) is indicative of the adsorption of hydrocarbon fragments, whereas the features below 1500 cm^{-1}, corresponding to the C—C stretch, and CH_2 vibrations (scissors, wag, twist, and rock) as well as the Si—C stretch [26], cannot be resolved. In the case of ion irradiation in ethylene at 200 eV impact energy, Fig. 8b shows, in addition to the generally more intense adsorption features, the presence of hydrogen adsorption as indicated by the strong features at 644 cm^{-1} (SiH bending mode), 893 cm^{-1} (SiH_2 scissoring mode), and 2075 cm^{-1} (Si—H stretching mode) [27]. The weak peak at 1387 cm^{-1} can be assigned to a CH_2 scissoring mode [26]. After the sample was annealed to 1000 K, all the hydrogen-related features disappeared, and only the peak near

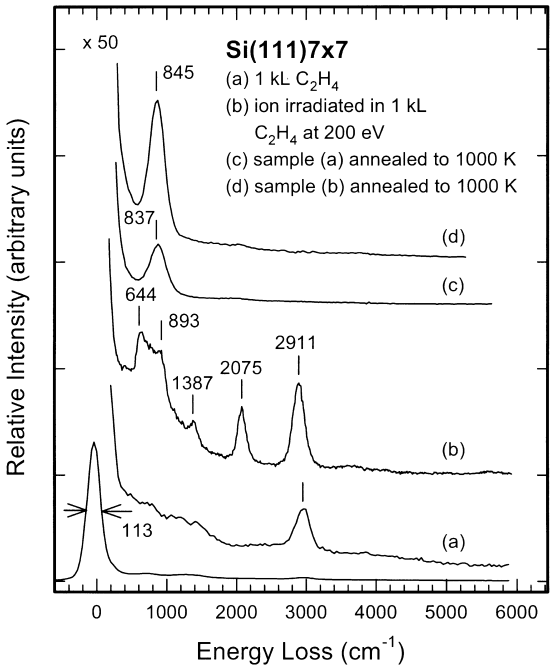

Fig. 8. Vibrational electron energy loss spectra for Si(111)7×7 (a) exposed with 1 kL of ethylene, (b) ion-irradiated with 1 kL of ethylene ions at 200 eV impact energy, both at 300 K, (c) sample (a) annealed to 1000 K, and (d) sample (b) annealed to 1000 K.

840 cm^{-1}, corresponding to Si—C stretch, remained (Fig. 8c and d). Evidently, the increase in the intensity of the peak at $\sim$840 cm^{-1} for the ion-irradiated sample suggests that production of surface carbon by ion-assisted reactions (Fig. 8d) could be significantly enhanced relative to that by thermal dissociation (Fig. 8c) [1].

Fig. 9 shows the electronic EELS spectra for surface carbon produced by ion irradiation in 10 kL of ethylene at 50 eV impact energy followed by annealing to 800 and 1270 K. The spectra for the ion-irradiated sample (Fig. 9a) before and after the 800 K anneal are characterized by a broad plasmon peak near 20 eV similar to that observed

[1] It should be noted that the difference in the peak location of the Si–C stretch observed in Figs. 5 and 8 may be due to the different deposition techniques (ion irradiation vs. thermal methods) that introduced a different degree of roughness in the prepared surface. More detailed investigations on the dependence of spectral features on the preparation conditions will be of interest.

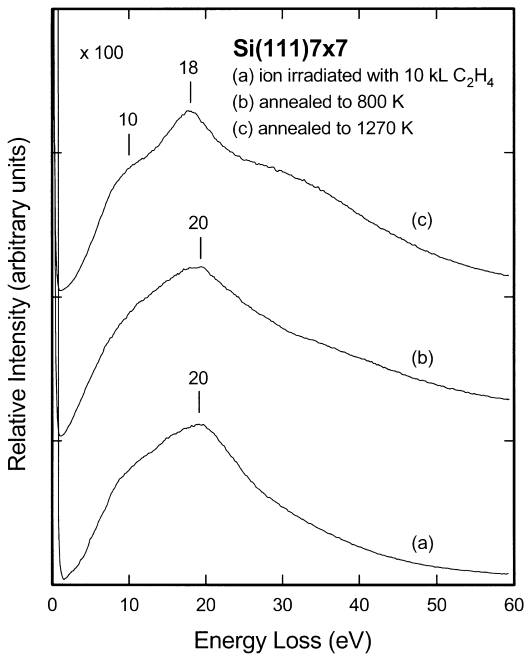

Fig. 9. Electronic electron energy loss spectra for Si(111)7 × 7 (a) ion-irradiated in 10 kL of ethylene at 50 eV impact energy, followed by annealing to (b) 800 K, and (c) 1270 K.

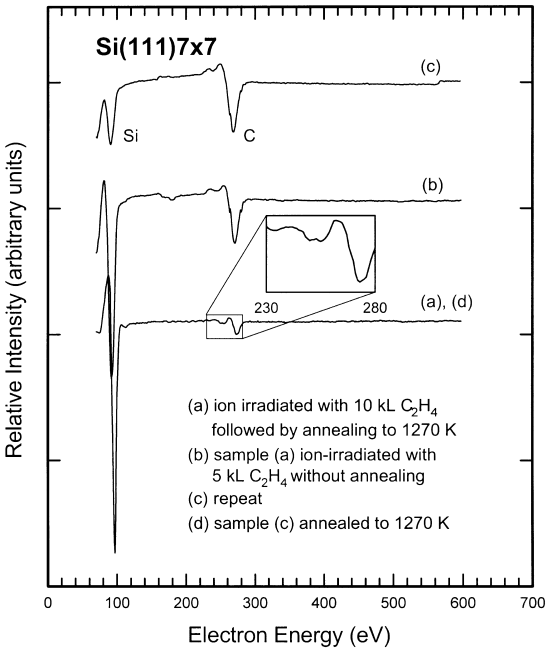

Fig. 10. Auger electron spectra for Si(111)7 × 7 (a) ion-irradiated in 10 kL of ethylene at 50 eV impact energy and annealing to 1270 K, (b) followed by ion irradiation with 5 kL of ethylene, and (c) sample (b) ion-irradiated with 5 kL of ethylene, all at 300 K, and (d) sample (c) annealed to 1270 K.

in the thermal deposition case (Fig. 7c). The carbonaceous layer so produced can therefore be assigned as a Si–C alloy, as discussed earlier. In Fig. 9a, specific contributions from the hydrogen-related species are not observed, which may be due to the close proximity of the plasmon peaks for the amorphous C:H and C species (Table 1). After the sample was further annealed to 1270 K (Fig. 9c), restoration of the clean silicon surface was indicated by the shift in the position of the bulk plasmon peak back to 18 eV (see, for example, Fig. 7a), which in turn suggests that diffusion of surface carbon into the bulk might have occurred.

The EELS results are consistent with the corresponding AES results shown in Fig. 10a, whereby carbon was clearly found in the near-surface region along with a prominent Si signal. However, further irradiation of the resulting sample by ethylene ions without subsequent annealing (Fig. 10b and c) reduced the Si signal but strengthened the C signal substantially, which indicates that the relative carbon concentration continues to increase with increasing ethylene ions dosage. It is of interest to note that annealing the resulting sample shown in Fig. 10c to 1270 K again restored the previous sample condition shown in Fig. 10a, which suggests that carbon did not remain at the top layer of the substrate but diffused into the bulk. This diffusion process may provide an efficient way of generating a uniform SiC layer in the sub-surface region [15]. In the previous studies [28,29], the line shape of the carbon KLL Auger peak has been used to determine the different types of bonding in carbon (graphite, diamond, and SiC). Fig. 11 illustrates the differences in the line shapes for the carbon KLL Auger lines in the 240–270 eV region for graphite (sp^2), natural diamond (sp^3), and SiC, as reported in Refs. [28,29]. In our spectrum (insert of Fig. 10a), the line shape of the carbon KLL peak clearly supports the existence of SiC.

Although the diffusion of carbon into the bulk has been observed by using thermal and ion-assisted deposition methods, it has not been found to occur at a very high dosage of ethylene ions.

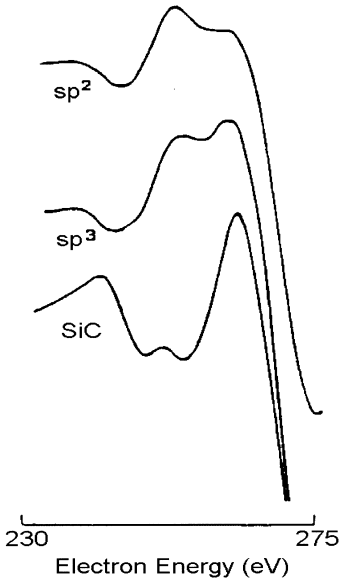

Fig. 11. Typical carbon KLL Auger lines of graphite (sp^2), natural diamond (sp^3), and SiC (after Refs. [25,26]).

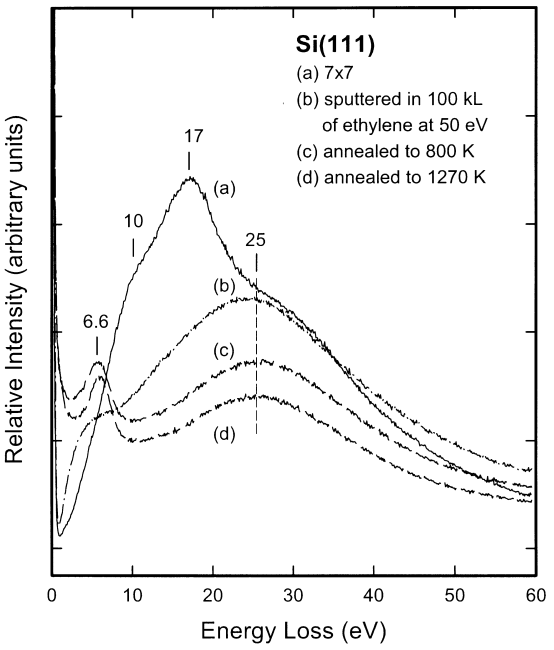

Fig. 12. Electronic electron energy loss spectra for (a) clean Si(111)7×7, (b) sputtered in 100 kL of ethylene at 50 eV impact energy, followed by annealing to (c) 800 K, and (d) 1270 K.

Fig. 12 shows the electronic EELS spectra of Si(111)7×7 ion-irradiated with 100 kL of ethylene at 50 eV impact energy at RT followed by annealing to 800 and 1270 K. In considering the typical energy positions of the plasmon peaks listed in Table 1, the broad shoulder at 6.6 eV shown in Fig. 12b could correspond to a mixture of different carbon bonding structures including *a*-C, *a*-C:H, and graphite. The presence of the broad $\pi+\sigma$ plasmon peak at 25 eV suggests that the dominant species was graphite. Although the $\pi+\sigma$ plasmon for *a*-C:H also locates at 25 eV, it is unlikely that *a*-C:H could remain intact after annealing to 1270 K because hydrogen would desorb during the high-temperature anneal. The sharpening of the π plasmon peak at 6.6 eV after annealing the sample to 800 K (Fig. 12c) is consistent with hydrogen desorption from the surface and recombination of carbon atoms to form a graphite layer. Once the graphite was formed on the surface, however, annealing the sample further to a higher temperature (1270 K in Fig. 12d) did not cause the carbon to undergo further diffusion into the bulk. To confirm the formation of graphite on the surface, Fig. 13 shows the corresponding AES spectra for the sample after ethylene ions irradiation before (Fig. 12b) and after the 1270 K anneal (Fig. 12d). Both spectra (Fig. 13a and b) exhibit a strong carbon peak and a relatively weak silicon peak. Unlike the case of a smaller dosage of ethylene ions shown in Fig. 10, annealing the present sample to 1270 K did not change the relative intensity ratio of the carbon to silicon peaks. However, the line shape of the carbon KLL Auger line changed from an irregular shape (Fig. 13c) to that of a typical graphite line shape after annealing (Fig. 13d). The irregular line shape in Fig. 13c could be caused by 'mixed' contributions from graphite, Si–C alloy and other hydrocarbon species. A high exposure of ethylene ions at RT therefore appears to cause the formation of graphite, which in turn prevents the diffusion of carbon into the bulk and hence the formation of SiC.

4. Summary

In the present work, we investigated the initial film growth processes involved in the formation

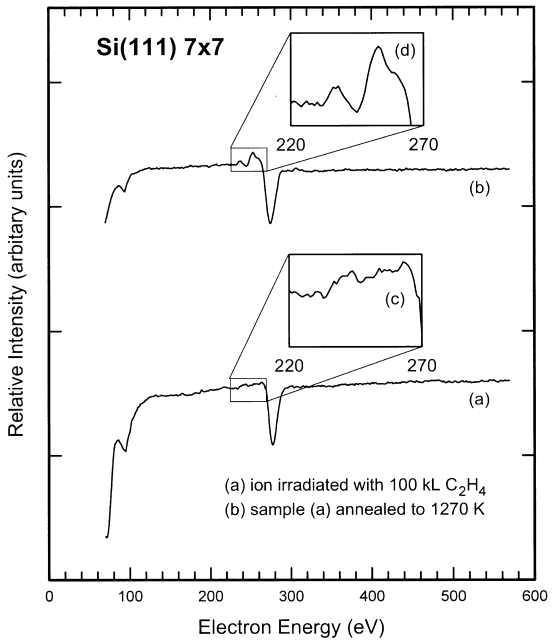

Fig. 13. Auger electron spectra for Si(111)7×7 (a, c) ion-irradiated in 100 kL of ethylene at 50 eV impact energy, followed by (b, d) annealing to 1270 K.

of SiO_2 and SiC layers on Si(111)7×7 by using vibrational and electronic EELS, as well as AES. The SiO_2 layer can be obtained by annealing the silicon sample in O_2 at 700 K, and its presence is characterized by its electronic transitions near 5 and 7 eV. The formation of SiO_2 can also be obtained non-thermally by ion irradiation in oxygen at RT. For the formation of a carbonaceous layer, we verified that the formation of the so-called Si–C alloy on the surface can also be achieved thermally by annealing Si(111)7×7 in ethylene at 800 K and that diffusion of carbon atoms into the bulk occurs at a higher temperature (1270 K). Furthermore, like the formation of SiO_2, a higher efficiency in producing the carbonaceous layer could be achieved by using ion-assisted deposition than with thermal deposition. A very large dosage of ethylene ions (100 kL) at RT was found to cause the formation of a graphite layer, which prevented the diffusion of carbon into the bulk and hence the formation of the SiC layer. In future studies, it would be of great interest to determine the quality and morphology of these films as a function of the ion irradiation parameters and to further explore other more efficient methods of producing a uniform and better-defined carbonaceous layer on silicon surfaces. For instance, other growth procedures such as diluting hydrocarbons with a large proportion of hydrogen (99%) as the reactant gas have been found to be critical in producing diamond or diamond-like carbon films [9]. In the present work, electronic EELS experiments covering a wide energy loss range together with high-resolution vibrational EELS studies have proven to be a powerful combination for chemical-state composition analysis and surface bonding determination of the near-surface and surface regions. Further applications of this kind of 'combined' electronic and vibrational EELS investigation would help to improve our understanding of these important film growth processes for technological materials.

Acknowledgement

This work was supported by the Natural Sciences and Engineering Research Council of Canada.

References

[1] G. Hollinger, F.J. Himpsel, Phys. Rev. B 28 (1983) 3651.
[2] G. Comtet, L. Hellner, G. Dujardin, M.J. Ramage, Surf. Sci. 352–354 (1996) 315.
[3] R. Martel, Ph. Avouris, I.W. Lyo, Science 272 (1996) 385.
[4] H. Ibach, N.D. Bruchmann, H. Wagner, Appl. Phys. A 29 (1982) 113.
[5] M. Green, A. Liberman, J. Phys. Chem. Solids 23 (1962) 1407.
[6] G. Hollinger, Y. Jugnet, T.M. Duc, Solid State Commun. 22 (1977) 277.
[7] H. Ibach, J.E. Rowe, Phys. Rev. B 9 (1974) 1951.
[8] P. Kovarik, E.B.D. Bourdon, R.H. Prince, Phys. Rev. B 48 (1993) 12123.
[9] J.C. Augus, Thin Solid Films 216 (1992) 126.
[10] M. Ohring, The Materials Science of Thin Films, Academic Press, Toronto, 1992.
[11] J.W. Rabalais (Ed.), Low Energy Ion–Surface Interactions, Wiley, Baffins Lane, 1994.
[12] J.J. Cuomo, S.M. Rossnagel, H.R. Kaufman (Eds.), Handbook of Ion Beam Processing Technology, Noyes Publications, Park Ridge, 1989.

[13] H. Ibach (Ed.), Electron Spectroscopy for Surface Analysis, Springer, New York, 1977.
[14] M.P. Seah, W.A. Dench, Surf. Interf. Anal. 1 (1979) 2.
[15] F. Bozso, J.T. Yates Jr., W.J. Choyke, L. Muehlhoof, J. Appl. Phys. 57 (1985) 2771.
[16] D.Q. Hu, Ph.D. thesis, University of Waterloo, Waterloo, 1993.
[17] H. Yu, D.Q. Hu, K.T. Leung, J. Vac. Sci. Technol. A 15 (1997) 2653.
[18] Eight Peak Index of Mass Spectra Vol. 1, Mass Spectrometry Data Center, Aldermaston, 1974.
[19] H. Froitzheim, I. Ibach, D.L. Mills, Phys. Rev. B 11 (1975) 4980.
[20] E.C. Samano, G. Soto, J. Valenzuela, L. Cota, J. Vac. Sci. Technol. A 15 (1997) 2585.
[21] M. Tabe, T.T. Chiang, I. Lindau, W.E. Spicer, Phys. Rev. B 34 (1986) 2706.
[22] H. Froitzheim, D.A. King, D.P. Woodruff (Eds.), The Chemical Physics of Solid Surfaces and Heterogeneous Catalysis Vol. 5, Elsevier, New York, 1988, p. 202.
[23] E.A. Taft, H.R. Phillip, Phys. Rev. A 138 (1965) 197.
[24] Y. Ohno, Phys. Rev. B 39 (1988) 8209.
[25] P.A. Taylor, M. Bozack, W.J. Choyke, J.T. Yates Jr., J. Appl. Phys. 65 (1989) 1099.
[26] J. Yoshinobu, H. Tsuda, M. Onchi, M. Nishijinma, Solid State Commun. 60 (1986) 801.
[27] H. Froitzheim, U. Kohler, H. Lammering, Surf. Sci. 149 (1985) 537.
[28] A.K. Green, V. Rehn, J. Vac. Sci. Technol. A 1 (1983) 1877.
[29] Y.W. Ko, S.I. Kim, J. Vac. Sci. Technol. A 15 (1997) 2750.